Adsorption of Volatile Organic Compounds Onto Biomass-Derived Activated Carbons: Experimental Measurement and Comparison

Tahmid Hasan Rupam
Kyushu University Program
for Leading Graduate School,
Green Asia Education Center, Kyushu University,
Kasuga-koen 6-1, Kasuga-shi,
Fukuoka 816-8580, Japan
e-mail: rupam.tahmid.hasan.226@m.kyushu-u.ac.jp

Bidyut Baran Saha[1]
International Institute for Carbon-Neutral Energy Research (WPI-I2CNER),
Kyushu University,
744 Motooka, Nishi-ku,
Fukuoka 819-0395, Japan;
Department of Mechanical Engineering,
Kyushu University,
744 Motooka, Nishi-ku,
Fukuoka 819-0395, Japan
e-mail: saha.baran.bidyut.213@m.kyushu-u.ac.jp

Mujib L. Palash
Department of Electrical and Electronic Engineering,
University of Dhaka,
Dhaka 1000, Bangladesh
e-mail: mlpalash@du.ac.bd

Animesh Pal
Department of Nuclear Engineering,
University of Dhaka,
Dhaka 1000, Bangladesh
e-mail: animeshpal@du.ac.bd

Volatile organic compounds (VOCs) are a class of hazardous gaseous materials emitted from certain solids or liquids. They are thought to possess serious short- or long-term adverse effects on human health. Nowadays, an energy-efficient and cost-effective volatile organic compound removal system is of absolute necessity due to its adverse effects. In this regard, solar or waste heat-driven adsorption-based technologies can provide an energy-efficient system; however, most of the time, their utilization is limited by the high cost of the adsorbent materials. Right now, only one commercial high-grade activated carbon named Maxsorb III is known to have high capturing capacities. The purchasing cost of this adsorbent is very high, and it is derived from a non-renewable source. Therefore, this study is intended for the quest for low-priced biomass-derived activated carbons for an energy-efficient and cost-effective VOCs removal system. Two biomass-derived activated carbons synthesized from mangrove wood and waste palm trunk precursors are chosen, and four types of VOCs (ethanol, dichloromethane, acetone, and ethyl acetate) adsorption onto them are measured experimentally using the inverse gas chromatography technique. The zero uptake adsorption enthalpy and specific entropy of the adsorption are theoretically computed for all the adsorbent/adsorbate pairs. After that, these data are compared with the obtained data for Maxsorb III to assess the performance of the biomass-derived activated carbons. Results show that, for all the VOCs, the cost-effective mangrove-based activated carbon can be an excellent alternative to the high-priced Maxsorb III when employed as an adsorbent material for VOCs removal. [DOI: 10.1115/1.4055182]

Keywords: activated carbon, adsorption, biomass, inverse gas chromatography, volatile organic compounds, advanced materials and processing, alternative energy system design, environment, heat and mass transfer, smart materials, thermal analysis, thermal systems

1 Introduction

According to Environmental Protection Agency, volatile organic compounds (VOCs) are defined as "any compound of carbon, excluding carbon monoxide, carbon dioxide, carbonic acid, metallic carbides or carbonates, and ammonium carbonate, which participates in atmospheric photochemical reactions" [1]. These organic pollutants possess high vapor pressure at room temperature and directly impact human health and the environment.

With the persistent increase of VOCs and their harmful impact on human health and the ecological environment, stringent emission regulation of the Goteborg protocol was proposed in 1999 [2,3]. Therefore, developing an effective VOCs elimination technique is of great significance and urgent. Consequently, extensive efforts have been made in recent years to develop efficient VOC removal techniques, and many removal techniques have emerged. It can be commonly divided into destruction and recovery methods based on whether the VOCs can be recovered [1]. The recovery methods include adsorption, absorption, membrane separation, and condensation, whereas the destruction techniques include plasma catalysis, incineration, ozone catalytic oxidation, biological degradation, photocatalytic oxidation, etc. Among all these techniques, adsorption is considered as one of the most promising methods to treat VOCs as a highly efficient and economically somehow viable control strategy since it has the potential to recover and reuse both adsorbent and adsorbate. The characteristics of VOCs removal techniques are summarized in Table 1.

The solid porous adsorbent is a crucial element for VOC removal using the adsorption process [4]. Adsorbents such as activated carbon (AC), AC fiber, metal-organic frameworks, and zeolite have been widely studied materials [4,11–15]. Among them, AC is known to have the most potential as a low-cost, high-efficiency, acid/base- and thermo-stability adsorbent for VOCs removal [4]. Literature studies show that VOCs adsorption capacity onto different ACs ranges from 15.9 mg g^{-1} to several hundreds of milligrams per gram [4,11–13,16]. The key factors that influence the VOCs adsorption performance onto ACs are physicochemical properties such as large specific surface area, rich porous structure, pore volume, surface chemical functional groups, etc., properties of adsorbates (VOCs) such as molecular size and the polarity, as well as the adsorption conditions such as temperature, moisture, etc.

However, finding the optimal porous activated carbon in terms of cost and its physicochemical properties is crucial for the commercial application of the adsorption technique. Therefore, in this study, two activated carbons (M-AC (mangrove wood derived activated carbon) and WPT-AC (waste palm truck derived activated carbon)) synthesized from waste mangrove wood, and palm trunk biomass precursors are chosen, and four types of VOCs (ethanol, dichloromethane, acetone, and ethyl acetate) adsorption onto them are experimentally investigated at three different temperatures

[1]Corresponding author.

Manuscript received November 9, 2021; final manuscript received August 1, 2022; published online August 22, 2022. Assoc. Editor: Dr. Chun Yang.

Table 1 Characteristics of different VOCs removal techniques [4]

Method	Commercialize	Efficiency	Secondary waste generation	Energy consumption	Reuse	Reference
Adsorption	High	>90%	Spent adsorbent	Moderate	Yes	[5]
Condensation	High	Moderate	–	High	Yes	[6]
Incineration	High	>99% (40 min)	CO, NO*x*	Moderate	No	[6]
Absorption	Low	–	Spent absorbent	Moderate	Yes	[4]
Membrane separation	Not widely commercialized	–	Clogged membranes	High	Yes	[6]
Plasma catalysis	Not widely commercialized	74–81%	Formic acid, carboxylic acids, NO*x*, O_3	High	No	[7]
Biological degradation	Not widely commercialized	100% (~7 months)	Acetaldehyde, propanol, acetone	Low	No	[8]
Photocatalytic oxidation	Low-moderate	100% (5 min)	Strong oxidant OH radicals	Moderate	No	[9]
Ozone catalytic oxidation	High	100% (2 h)	Secondary organic aerosols	High	No	[10]

employing the inverse gas chromatography (IGC) technique. The zero uptake adsorption enthalpy and specific entropy of the adsorption are also theoretically computed for all the samples. Here, the first one accounts for the heat generated from the exothermic physical adsorption, whereas the second term specifies the driving force to provide a connection amid the equilibrium and non-equilibrium conditions of an adsorption system [17,18]. After that, these data are compared with the obtained data under identical conditions for a typical commercial activated carbon Maxsorb III made from petroleum coke.

2 Materials

In this study, three types of activated carbons, Maxsorb III, WPT-AC, and M-AC, were used as adsorbent material. Among these samples, Maxsorb III was commercially purchased from the Kansai Coke and Chemical. Co. Ltd, Japan; and M-AC and WPT-AC were synthesized from two biomass sources, namely, mangrove wood and waste plum trunk, respectively. The dried biomasses with their elemental analysis prior to the activation are given in Fig. 1 and Table 2, respectively. At first, the biomass sources were washed, dried, and crushed into smaller pieces. After that, the biomasses were carbonized and then activated with potassium hydro-oxide. After the activation, samples were rewashed again with hydrochloric acid and deionized water to get the final product. The detailed synthesis procedures can be found in the literature provided by Pal [19].

The porous properties of these samples have been investigated in previous studies utilizing the nitrogen adsorption/desorption experiment at 77 K using the volumetric adsorption equipment "3Flex™ Surface Characterization Analyzer" developed by Micromeritics Instrument Corp., USA. The porous properties of the studied samples are summarized in Table 3. The activated carbons selected in this study have high Brunauer, Emmett, and Teller (BET) surface areas in the range of 3000 $m^2\ g^{-1}$ with an average pore size residing in the microporous region. The elemental analysis data of the studied activated carbons are furnished in Table 4.

VOCs come from both anthropogenic sources such as exploitation, storage, refining, transport, and usage of fossil fuels and natural sources such as terrestrial and ocean. The emission of VOCs has been increasing intensely owing to the development of industries [4]. VOCs are more than 300 types of carbon-based chemicals, and all generally have a low boiling point, high vapor pressure, and strong reactivity, especially concerning photochemical reactions [4]. It is harmful to humans and the environment. As for human health, alcohols, halogenated VOCs, ketones, and aromatic compounds are toxic and carcinogenic [23]. This study focuses on the henry region adsorption of four different VOCs, namely, ethyl acetate, dichloromethane, acetone, and ethanol. The

Fig. 1 Pictorial view of dried biomass sources [19]

Table 2 Elemental analysis of the dried biomasses prior to the activation

Sample name	C (%)	H (%)	N (%)	O (diff.) (%)	Ash (%)	Reference
M-AC	46.70	6.04	0.14	45.98	1.14	[19]
WPT-AC	44.02	5.75	0.49	48.41	1.33	[19]

Table 3 Porous properties of the studied activated carbons

Sample name	BET surface area ($m^2\ g^{-1}$)	Total pore volume ($cm^3\ g^{-1}$)	Average pore width (nm)	Reference
Maxsorb III	3299	1.72	1.11	[20]
M-AC	2924	2.18	1.47	[21]
WPT-AC	2927	2.51	1.68	[21]

Table 4 Elemental compositions of the studied activated carbons

Sample name	C (%)	H (%)	N (%)	O (diff.) (%)	Ash (%)	Reference
Maxsorb III	95.13	0.14	0.25	4.35	0.13	[22]
M-AC	94.91	0.00	0.13	4.96	–	[19]
WPT-AC	92.61	0.04	0.10	7.08	0.17	[19]

Table 5 Physiochemical properties of the studied VOCs [24,25]

VOCs	Ethyl acetate	Acetone	Dichloromethane	Ethanol
Chemical formula	$CH_3COOCH_2CH_3$	$(CH_3)_2CO$	CH_2Cl_2	CH_3CH_2OH
Molar mass (kg kmol^{-1})	88.11	58.08	84.93	46.068
Critical temperature (°C)	250.55	234.95	235.05	241.56
Critical pressure (kPa)	3880	4700	6350	6268
Normal boiling point (°C)	77.10	56.07	40	78.42
Triple point temperature (°C)	−83.90	−94.65	–	−114.15

physiochemical properties of the VOC adsorbates are tabulated in Table 5.

3 Research Methodology

This study includes two major parts: selection of biomass-derived high-grade activated carbons and then using those carbons as adsorbents materials for the studied VOC adsorption. Additionally, the assorted VOC adsorptions onto commercial activated carbon, Maxsorb III, were obtained under similar conditions for comparison purposes. After obtaining the (infinite dilution) experimental adsorption data, the Henry constant of the studied pairs were obtained using Henry's adsorption isotherm model. Using the values of Henry's constant at different temperatures, the minimum regeneration temperatures for the activated carbon/VOC pairs were calculated. Additionally, the thermodynamic quantities, namely, adsorption enthalpy and specific entropy at the Henry's law region, were analyzed. The whole procedure of the workflow is given in Fig. 2.

4 Theory and Experiment

Adsorbate uptakes onto activated carbons in Henry's law region were measured by the IGC technique using the inverse gas chromatography-surface energy analyzer (IGC-SEA) (Surface Measurement System Ltd, UK). The IGC-SEA unit is equipped with two sample column holders along with 12 slots for solute reservoirs where the adsorbates are kept in a liquid phase. In this study, we have used four slots for four different VOCs. The experimental setup also includes an inbuilt oven to maintain its temperature (from 20 °C to 150 °C). The IGC-SEA also features a flame ionization detector (FID), mass flow controllers, and a processing unit for controlling and data analysis.

Figure 3 depicts the schematic diagram of the experimental unit. During the experiment, activated carbon samples were placed inside the 3 mm-sized sterilized glass columns. Then, controlled amount of one of the adsorbates with different concentrations was purged at a constant temperature inside the column with the help of carrier gas. In this case, the carrier gas was helium. After adsorption, the adsorbed adsorbate was swept away (desorbed) by the same carrier gas and detected at the outlet using the FID. Using the analysis software provided by the Surface Measurement System Ltd., UK, the respective chromatographs were constructed. The chromatographic data can be invoked to obtain the retention time and retention volume for the respective adsorbate. This unique characteristic of inverse gas chromatography enables it to successfully determine the experimental adsorption uptake in Henry's region.

To calculate the partial pressure, the height and area of the chromatographic curve are used. The governing equation can be written as [26,27]

$$P = \frac{n_{ads} \times R \times H_{Peak} \times 273.15}{F \times A} \tag{1}$$

Here, n_{ads} is the mole number of the purged adsorbate, R is the universal gas constant, F is the carrier gas flowrate, and H_{Peak} and A stand for the peak height and area of the recorded chromatographs.

At a specific partial pressure P, the adsorbed amount of VOC can be obtained by the following equation [28,29]:

$$n_{VOC} = \frac{1}{R \times T} \int_0^P V_n dP \tag{2}$$

where V_n is the retention volume obtained from the chromatographic data using the below given equation [30–32]:

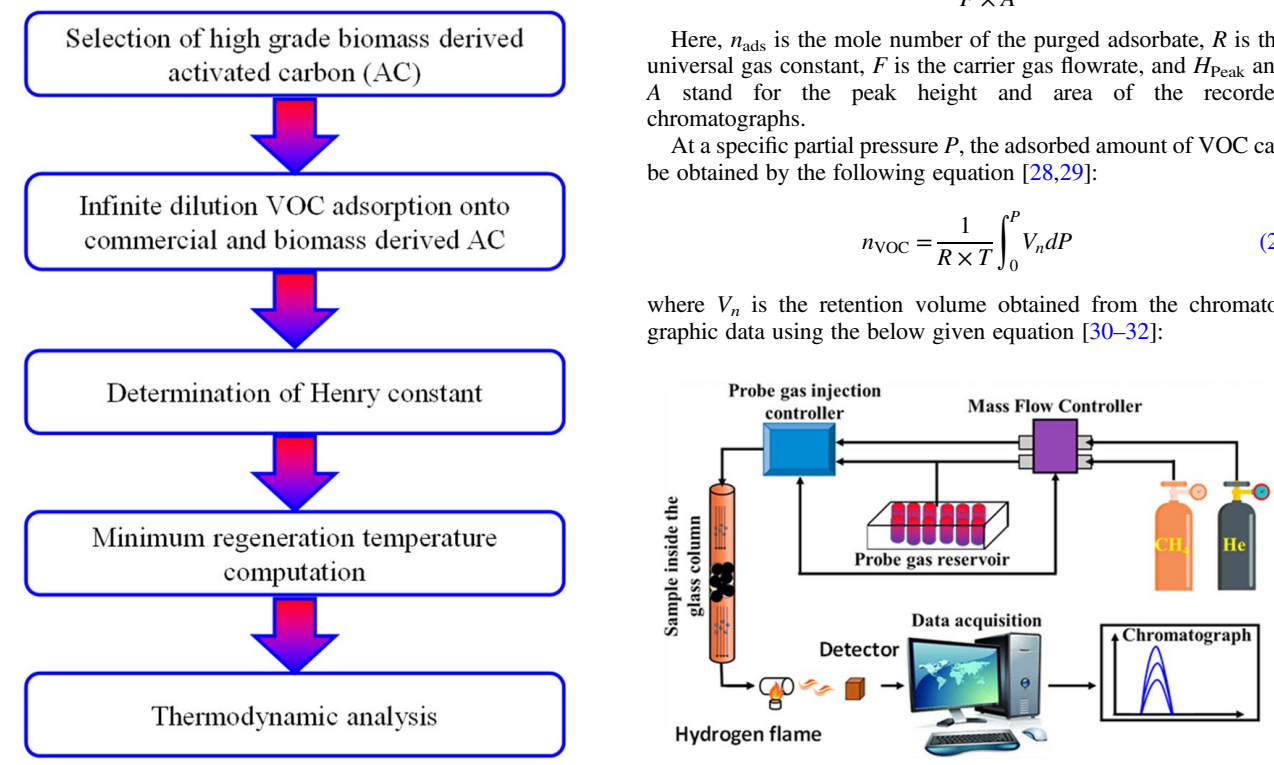

Fig. 2 Scheme of research methodology

Fig. 3 Schematic diagram of the IGC-SEA experimental unit

$$V_n = jF(t_R - t_0)$$

Here, j is the James–Martin correction factor, and t_R and t_0 stand for the retention time and the dead time, respectively [33,34].

Data obtained from Eqs. (1) and (2) are used to calculate the adsorption isotherms for the studied adsorption pairs. Once the adsorbate uptake at different pressures at a constant temperature in Henry's law region is obtained, it is possible to construct the Henry region adsorption isotherms for the selected VOCs. After that, the isotherm data can be correlated with the Henry isotherm model given in Eq. (3) to specify the respective Henry constants, K_H. The Henry isotherm model has the following mathematical form:

$$W = K_H \times P \tag{3}$$

Here, W is the adsorbate loading in kg kg^{-1}, and P is the partial pressure of the adsorbate gas.

The Henry constant can be utilized to obtain the zero uptake adsorption enthalpy (Δh^0) of the respective adsorbent/adsorbate pairs using the Clausius–Clapeyron relationship given in Eq. (4).

$$\Delta h^0 = R\left[\frac{\partial(\ln K_H)}{\partial(1/T)}\right] \tag{4}$$

This zero uptake adsorption enthalpy or isosteric heat of adsorption is defined as the released heat during the formation of exothermic Van der Walls bonds in physical adsorption and can be expressed by the opposing enthalpic and entropic effects using the following expression [35]:

$$\Delta h^0 = T\Delta s^0 - \Delta g^0$$

Here, Δg^0 and Δs^0 are the changes in Gibbs free energy in kJ kg^{-1} and change in adsorbed phase entropy in kJ kg^{-1} K^{-1}, respectively, due to adsorption. This Gibbs free energy has two parts: one relating to the changes in chemical potential of the adsorbate (μ_g) while the other involves the grand potential of the solid adsorbent (Ω_s) [36]. Neglecting the changes of solid grand potential, the zero uptake isosteric heat of adsorption in the Henry's law region can be found as

$$\Delta h^0 = T\Delta s^0 - \mu_g$$

$$\Rightarrow T\Delta s^0 = \Delta h^0 + RT\ln\left(\frac{P^0}{P^*}\right) \tag{5}$$

where $\mu_g = RT \ln P^*/P^0$ is the chemical potential of the adsorbate gas, P^0 stands for the saturated pressure of the bulk gas phase, while P^* is the fugacity of the gas reference. At Henry's law region, $P^* = P$, where P is the gas pressure as the gas would behave like an ideal gas. Therefore, invoking the equation of state for the ideal gas, it can be written as

$$P^0 V_p = n_{\mathrm{VOC}} RT$$

$$P^0 = \frac{n_{\mathrm{VOC}} RT}{V_P}$$

Here, V_p is the volume in the pores. In the infinite dilution adsorption region, the adsorption isotherm is modeled using Henry's adsorption isotherm model. This model predicts a linear relation

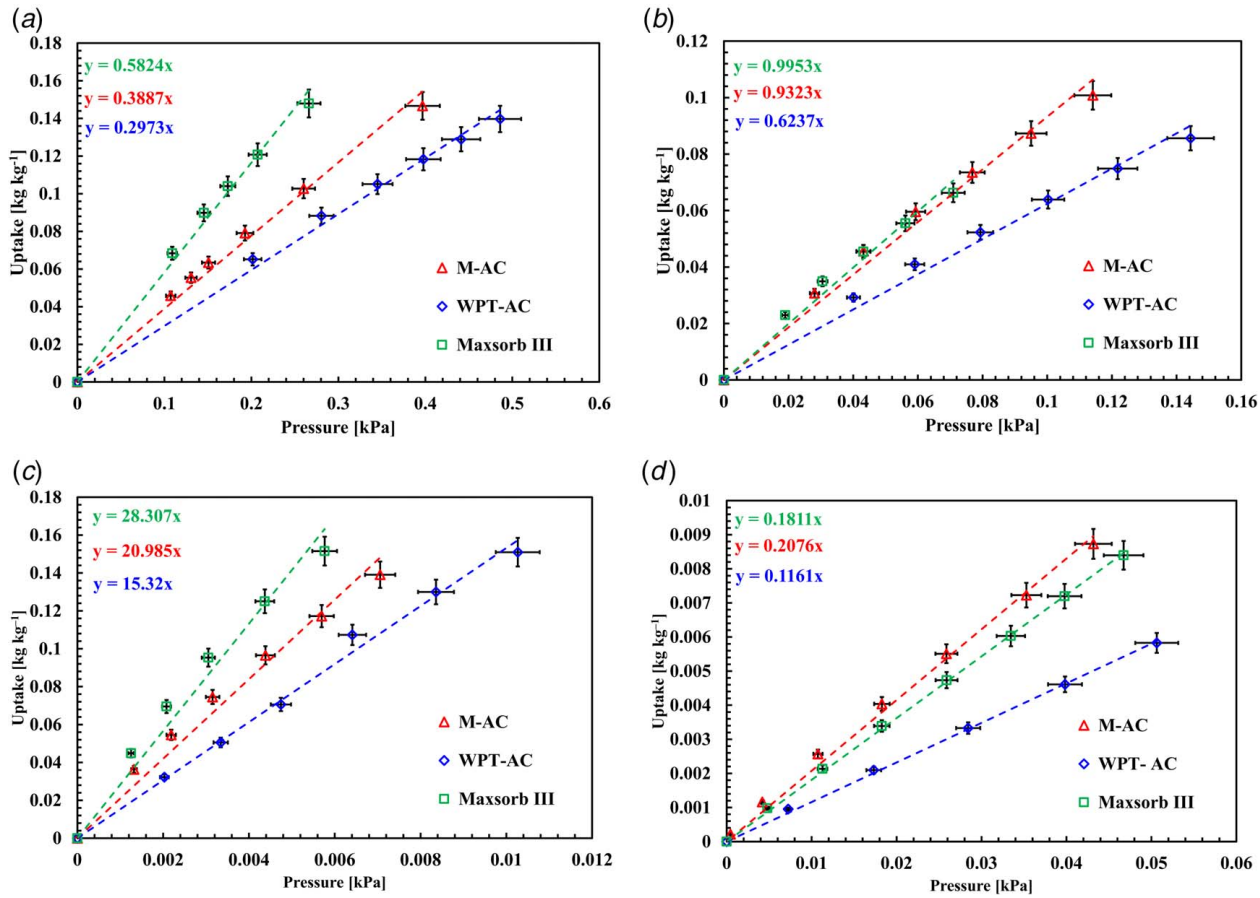

Fig. 4 Adsorption isotherms of (*a*) dichloromethane, (*b*) acetone, (*c*) ethyl acetate, and (*d*) ethanol onto different activated carbons at 30 °C (experimental data points are given with ±5% error bars)

between adsorbate uptake with increasing vapor pressure.

$$W = K_H P$$

where K_H is Henry's constant.

Assuming that Henry's isotherm model is applicable for the whole pressure region, the maximum uptake can be obtained as

$$W_{\max} = K_H P^0$$

where P^0 is the saturation pressure of the adsorbate for a given adsorption temperature. Therefore, $W/W_{\max}$ is proportional to P/P^0.

Moreover,

$$\frac{P}{P^0} = \frac{n_{\mathrm{VOC}} RT}{V_p} \times \frac{K_H}{W} = \frac{n_{\mathrm{VOC}} RT}{V_p} \times \frac{K_H}{n_{\mathrm{VOC}}/M_s}$$

$$\Rightarrow \frac{P^0}{P} = \frac{K_H RT}{V_P}$$

Here, V_p is a specific pore volume. Equation (5) can be rewritten as

$$T\Delta s^0 = \Delta h^0 + RT \ln\left(\frac{K_H RT}{\upsilon_P}\right)$$

Table 6 Henry constant values for all the studied pairs

Adsorbate / Adsorbent	Henry constant, K_H (kg kg^{-1} kPa^{-1})											
	Dichloromethane			Acetone			Ethyl acetate			Ethanol		
	30 °C	50 °C	70 °C	30 °C	50 °C	70 °C	30 °C	50 °C	70 °C	30 °C	50 °C	70 °C
Maxsorb III	0.582	0.179	0.085	0.995	0.351	0.144	28.31	7.40	3.52	0.18	0.04	0.01
M-AC	0.389	0.157	0.098	0.932	0.267	0.117	20.99	5.08	2.41	0.20	0.05	0.02
WPT-AC	0.111	0.051	0.041	0.593	0.194	0.133	15.32	2.53	1.20	0.12	0.03	0.01

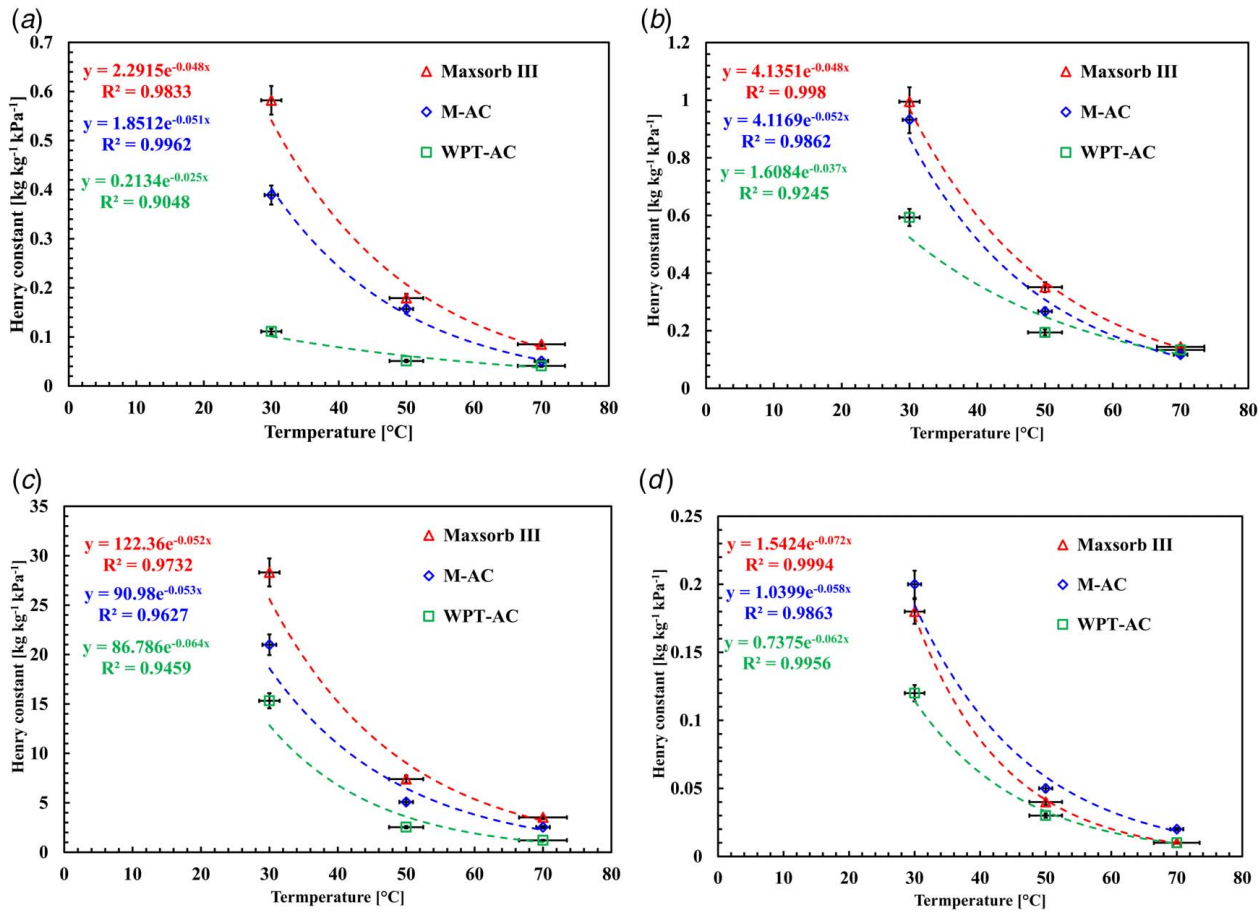

Fig. 5 Henry's constant as a function of adsorption temperature for (*a*) dichloromethane, (*b*) acetone, (c) ethyl acetate, and (*d*) ethanol adsorption onto different activated carbons (experimental data points are given with ±5% error bars)

Table 7 Minimum required regeneration temperatures

Conditions of regeneration	VOC / AC	Minimum required regeneration temperature (°C)			
		Dichloromethane	Acetone	Ethyl acetate	Ethanol
Complete regeneration at $K_h = 0.001$	Maxsorb III	161.18	173.48	225.28	101.96
	M-AC	147.50	160.05	215.44	118.42
	WPT-AC	214.50	199.54	177.68	106.50
Practical regeneration at $K_h = 0.01$	Maxsorb III	113.22	125.51	181.00	69.98
	M-AC	102.37	115.77	171.99	80.07
	WPT-AC	122.42	137.31	141.70	69.37

Table 8 Thermodynamic parameters for ACs/VOCs pairs

Adsorbate / Adsorbent	Dichloromethane		Acetone		Ethyl acetate		Ethanol	
	Δh^0 (kJ kg^{-1})	Δs^0 (kJ kg^{-1} K^{-1})	Δh^0 (kJ kg^{-1})	Δs^0 (kJ kg^{-1} K^{-1})	Δh^0 (kJ kg^{-1})	Δs^0 (kJ kg^{-1} K^{-1})	Δh^0 (kJ kg^{-1})	Δs^0 (kJ kg^{-1} K^{-1})
Maxsorb III	41.73	0.68	41.72	0.87	45.24	0.42	62.41	2.78
M-AC	29.99	0.306	45.02	1.09	46.99	0.54	49.89	1.95
WPT-AC	21.69	0.128	32.65	0.50	55.41	0.88	53.74	2.33

$$\Rightarrow \Delta s^0 = \frac{\Delta h^0}{T} + R \ln\left(\frac{K_H RT}{\upsilon_P}\right) \tag{6}$$

Equation (6) is used to calculate the adsorbed phase-specific entropy of ACs/VOCs pairs.

5 Results and Discussion

Four VOCs, namely, dichloromethane, acetone, ethyl acetate, and ethanol adsorption, onto three different activated carbons have been experimentally measured in the Henry region at three different temperatures of 30 °C, 50 °C, and 70 °C. For comparing the adsorption capacities, the isotherms obtained at 30 °C are given in Fig. 4. The determination of chromatographs at infinite dilution are quite accurate in IGC-SEA with a deviation of <0.8%. However, the system is also equipped with heaters and mass flowrate controllers which are associated with their respective errors. Therefore, the experimental data are given with a ±5% error bars. The Henry constant values for all the pairs are furnished in Table 6. From the isotherms, it can be concluded that for all the selected VOCs, the Maxsorb III type activated carbons exhibit the highest amount of VOCs loadings except for ethanol's case. M-AC type activated carbon shows higher ethanol adsorption compared with the other two activated carbons. Additionally, in the case of acetone adsorption, the adsorption uptake onto M-AC has negligible difference with Maxsorb III. Furthermore, in the case of dichloromethane and ethyl acetate, M-AC exhibits comparable VOCs uptakes with Maxsorb III. Nevertheless, in all cases, WPT-AC shows the lowest amount of adsorbate capturing capacity in Henry's law region.

It is evident from Table 6 that the values of Henry's constant decrease with increasing temperature, which is expected in the case of physical adsorption. In Fig. 5, Henry's constants as a function of adsorption temperature are plotted. It can be seen from Fig. 5 that for all the studied pairs, Henry's constants decreased exponentially with increasing temperatures. Using the exponential fitting equations, some useful information regarding the minimum temperature required for complete regeneration (Henry's constant is assumed to be 0.001 kg kg^{-1} kPa^{-1}) can be extracted. However, for practical application, the required regeneration can be obtained with Henry's constant value of 0.01 kg kg^{-1} kPa^{-1}. In both cases, the minimum desorption temperatures are calculated and are furnished in Table 7.

From Table 7, it can be seen that for dichloromethane and acetone, M-AC adsorbent would require the lowest regeneration temperature whereas, for ethyl acetate and ethanol, it is WPT-AC. On the other hand, in the case of dichloromethane and acetone, WPT-AC would require the highest amount of heat energy, and for ethanol and ethyl acetate, M-AC would consume the highest energy regarding regeneration. For all the adsorbates, Maxsorb III shows moderate requirements of regeneration temperatures. These regeneration temperatures depend on how the adsorbate molecules interact with the respective adsorbents' surfaces.

Using the isotherms data, the zero uptake adsorption enthalpy and specific entropy are computed employing Eqs. (4) and (6), respectively. The calculated data are furnished in Table 8. It can be seen that the enthalpy is lowest for WPT-AC/dichloromethane and acetone pairs, whereas the highest is observed for ethyl acetate adsorption onto WPT-AC. It is also noticed that among the three adsorbents/adsorbates pairs, Maxsorb III/ethanol shows the highest adsorption enthalpy and specific entropy. Generally, a larger pore volume for highly porous activated carbons results in more spaces for a single adsorbed molecule. Consequently, reduction in specific entropy is a result of the decreasing interaction among the adsorbed molecules [28].

6 Conclusions

Two activated carbons, namely, M-AC and WPT-AC made from mangrove wood and waste palm trunk biomass precursors, have been selected as potential adsorbents for VOCs adsorption. The four types of VOCs (ethanol, dichloromethane, acetone, and ethyl acetate) adsorption onto them are measured experimentally in the Henry region at three different temperatures of 30 °C, 50 °C, and 70 °C using the inverse gas chromatography technique. The obtained results are also compared with commercial activated carbon Maxsorb III tested under the same experimental conditions. The zero uptake adsorption enthalpy and specific entropy of the adsorption are theoretically calculated for all the samples. Results show that both activated carbons M-AC and WPT-ACs possess high adsorption performance of selected VOCs adsorption and are comparable with commercial activated carbon. M-AC type activated carbon shows higher ethanol adsorption compared with the other two activated carbons. Additionally, in the case of acetone adsorption, the adsorption uptake onto M-AC has negligible difference with Maxsorb III. Furthermore, in the case of dichloromethane and ethyl acetate, M-AC exhibits comparable VOCs uptakes with

Maxsorb III. Nevertheless, in all cases, WPT-AC shows the lowest amount of adsorbate capturing capacity in Henry's law region. Finally, it can be concluded that the cost-effective biomass-derived activated carbons can be very good alternatives to the high-priced Maxsorb III for adsorption-based VOCs removal systems.

Conflict of Interest

There are no conflicts of interest. This article does not include research in which human participants were involved. Informed consent not applicable. This article does not include any research in which animal participants were involved.

Data Availability Statement

The datasets generated and supporting the findings of this article are obtainable from the corresponding author upon reasonable request.

References

[1] Krishnamurthy, A., Adebayo, B., Gelles, T., Rownaghi, A., and Rezaei, F., 2020, "Abatement of Gaseous Volatile Organic Compounds: A Process Perspective," Catal. Today, **350**, pp. 100–119.

[2] Zhang, X., Gao, B., Zheng, Y., Hu, X., Creamer, A. E., Annable, M. D., and Li, Y., 2017, "Biochar for Volatile Organic Compound (VOC) Removal: Sorption Performance and Governing Mechanisms," Bioresour. Technol., **245**(A), pp. 606–614.

[3] Commission, U.N.E. Gothenburg Protocol.

[4] Zhang, X., Gao, B., Creamer, A. E., Cao, C., and Li, Y., 2017, "Adsorption of VOCs Onto Engineered Carbon Materials: A Review," J. Hazard. Mater., **338**, pp. 102–123.

[5] Jo, W. K., and Yang, C. H., 2009, "Granular-Activated Carbon Adsorption Followed by Annular-Type Photocatalytic System for Control of Indoor Aromatic Compounds," Sep. Purif. Technol., **66**(3), pp. 438–442.

[6] Luengas, A., Barona, A., Hort, C., Gallastegui, G., Platel, V., and Elias, A., 2015, "A Review of Indoor Air Treatment Technologies," Rev. Environ. Sci. Biotechnol., **14**(3), pp. 499–522.

[7] Hoeben, W. F. L. M., Beckers, F. J. C. M., Pemen, A. J. M., Van Heesch, E. J. M., and Kling, W. L., 2012, "Oxidative Degradation of Toluene and Limonene in Air by Pulsed Corona Technology," J. Phys. D: Appl. Phys., **45**(5), p. 055202.

[8] Lu, Y., Liu, J., Lu, B., Jiang, A., and Wan, C., 2010, "Study on the Removal of Indoor VOCs Using Biotechnology," J. Hazard. Mater., **182**(1–3), pp. 204–209.

[9] Yokosuka, Y., Oki, K., Nishikiori, H., Tatsumi, Y., Tanaka, N., and Fujii, T., 2009, "Photocatalytic Degradation of Trichloroethylene Using N-Doped TiO_2 Prepared by a Simple Sol-Gel Process," Res. Chem. Intermed., **35**(1), pp. 43–53.

[10] Hubbard, H. F., Coleman, B. K., Sarwar, G., and Corsi, R. L., 2005, "Effects of an Ozone-Generating Air Purifier on Indoor Secondary Particles in Three Residential Dwellings," Indoor Air, **15**(6), pp. 432–444.

[11] Li, L., Song, J., Yao, X., Huang, G., Liu, Z., and Tang, L., 2012, "Adsorption of Volatile Organic Compounds on Three Activated Carbon Samples: Effect of Pore Structure," J. Cent. South Univ., **19**(12), pp. 3530–3539.

[12] Borkar, C., Tomar, D., and Gumma, S., 2010, "Adsorption of Dichloromethane on Activated Carbon," J. Chem. Eng. Data, **55**(4), pp. 1640–1644.

[13] Oh, K.-J., Park, D.-W., Kim, S.-S., and Park, S.-W., 2010, "Breakthrough Data Analysis of Adsorption of Volatile Organic Compounds on Granular Activated Carbon," Korean J. Chem. Eng., **27**(2), pp. 632–638.

[14] Isinkaralar, K., Gullu, G., and Turkyilmaz, A., 2022, "Experimental Study of Formaldehyde and BTEX Adsorption Onto Activated Carbon From Lignocellulosic Biomass," Biomass Convers. Biorefinery.

[15] Ma, X., Yang, L., and Wu, H., 2021, "Removal of Volatile Organic Compounds From the Coal-Fired Flue Gas by Adsorption on Activated Carbon," J. Clean. Prod., **302**, p. 126925.

[16] Yu, F. D., Luo, L. A., and Grevillot, G., 2002, "Adsorbption Isotherms of VOCs Onto an Activated Carbon Monolith: Experimental Measurement and Correlation With Different Models," J. Chem. Eng. Data, **47**(3), pp. 467–473.

[17] Rupam, T. H., Islam, M. A., Pal, A., and Saha, B. B., 2020, "Adsorption Thermodynamics and Performance Indicators of Selective Adsorbent/Refrigerant Pairs," Appl. Therm. Eng., **175**, p. 115361.

[18] Pons, M., 1996, "Second Law Analysis of Adsorption Cycles With Thermal Regeneration," ASME J. Energy Resour. Technol., **118**(3), pp. 229–236.

[19] Pal, A., 2018, *Study on Novel Functional Activated Carbon and Composites for Adsorption Heat Pump Systems*, Kyushu University Library, Fukuoka, Japan.

[20] El-Sharkawy, I. I., Jing Ming, H., Ng, K. C., Yap, C., and Saha, B. B., 2008, "Adsorption Equilibrium and Kinetics of Gasoline Vapors Onto Carbon-Based Adsorbents," J. Chem. Eng. Data, **53**(1), pp. 41–47.

[21] Pal, A., Thu, K., Mitra, S., El-Sharkawy, I. I., Saha, B. B., Kil, H.-S., Yoon, S.-H., and Miyawaki, J., 2017, "Study on Biomass Derived Activated Carbons for Adsorptive Heat Pump Application," Int. J. Heat Mass Transfer, **110**, pp. 7–19.

[22] Uddin, K., El-Sharkawy, I. I., Miyazaki, T., Saha, B. B., Koyama, S., Kil, H. S., Miyawaki, J., and Yoon, S. H., 2014, "Adsorption Characteristics of Ethanol Onto Functional Activated Carbons With Controlled Oxygen Content," Appl. Therm. Eng., **72**(2), pp. 211–218.

[23] Patnaik, P., 2006, *A Comprehensive Guide to the Hazardous Properties of Chemical Substances*, 3rd ed., John Wiley & Sons, Inc., Hoboken, NJ.

[24] Lemmon, E. W., McLinden, M. O., and Huber, M. L., 2013, "Reference Fluid Thermodynamic and Transport Properties," NIST Standard Reference Data Base 23, Version 9.1.

[25] Chemical Database Provided by PubChem [Online], https://pubchem.ncbi.nlm.nih.gov, Accessed September 29, 2021.

[26] Ho, R., and Heng, J. Y. Y., 2013, "A Review of Inverse Gas Chromatography and Its Development as a Tool to Characterize Anisotropic Surface Properties of Pharmaceutical Solids," KONA Powder Part. J., **30**, pp. 164–180.

[27] Rupam, T. H., Palash, M. L., Chakraborty, A., and Saha, B. B., 2022, "Insights of the Adsorbents Surface Chemical Properties Effect on Water Adsorption Isotherms," Int. J. Heat Mass Transfer, **192**, p. 122842.

[28] Palash, M. L., Rupam, T. H., Pal, A., Chakraborty, A., Saha, B. B., and Wang, R., 2021, "Design Principles for Synthesizing High Grade Activated Carbons for Adsorption Heat Pumps," Chem. Eng. J. Adv., **6**, p. 100086.

[29] Cremer, E., and Huber, H., 1961, "Messung von Adsorptionsisothermen an Katalysatoren Bei Hohen Temperaturen Mit Hilfe Der Gas-Festkörper-Eluierungschromatographie," Angew. Chem., **73**(13), pp. 461–465.

[30] Pal, A., Kondor, A., Mitra, S., Thu, K., Harish, S., and Saha, B. B., 2019, "On Surface Energy and Acid–Base Properties of Highly Porous Parent and Surface Treated Activated Carbons Using Inverse Gas Chromatography," J. Ind. Eng. Chem., **69**, pp. 432–443.

[31] Mohammadi-Jam, S., and Waters, K. E., 2014, "Inverse Gas Chromatography Applications: A Review," Adv. Colloid Interface Sci., **212**, pp. 21–44.

[32] Schultz, J., and Martin, C., 1987, "The Role of the Interface in Carbon Fibre-Epoxy Composites," J. Adhes., **23**(1), pp. 45–60.

[33] Palash, M. L., Pal, A., Rupam, T. H., Park, B.-D., and Saha, B. B., 2020, "Surface Energy Characterization of Different Particulate Silica Gels at Infinite Dilution," Colloids Surfaces A Physicochem. Eng. Asp., **603**, p. 125209.

[34] Rupam, T. H., Palash, M. L., Islam, M. A., and Saha, B. B., 2022, "Transitional Metal-Doped Aluminum Fumarates for Ultra-Low Heat Driven Adsorption Cooling Systems," Energy, **238**, p. 122079.

[35] Prausnitz, J. M., 1990, "Molecular Thermodynamics for Chemical Process Design," Angew. Chem. Int. Ed. Engl., **29**(11), pp. 1246–1255.

[36] Myers, A. L., 2004, "Characterization of Nanopores by Standard Enthalpy and Entropy of Adsorption of Probe Molecules," Colloids Surfaces A Physicochem. Eng. Asp., **241**(1–3), pp. 9–14.